ZnO nanoparticles and nanowire array hybrid photoanodes for dye-sensitized solar cells

Supan Yodyingyong,[1,2] Qifeng Zhang,[1] Kwangsuk Park,[1] Christopher S. Dandeneau,[1] Xiaoyuan Zhou,[1] Darapond Triampo,[3] and Guozhong Cao[1,a)]
[1]*Department of Materials Science and Engineering, University of Washington, Seattle, Washington 98195, USA*
[2]*Institute for Innovative Learning, Mahidol University, 999 Phuttamonthon 4 Road, Nakhon Pathom 73170, Thailand*
[3]*Department of Chemistry, Center of Excellence for Innovation in Chemistry, Faculty of Science, Mahidol University, Bangkok 10400, Thailand*

(Received 6 January 2010; accepted 29 January 2010; published online 19 February 2010)

ZnO nanoparticle-nanowire (NP-NW) array hybrid photoanodes for dye-sensitized solar cell (DSC) with NW arrays to serve as a direct pathway for fast electron transport and NPs dispersed between NWs to offer a high specific surface area for sufficient dye adsorption has been fabricated and investigated to improve the power conversion efficiency (PCE). The overall PCE of the ZnO hybrid photoanode DSC with the N3-sensitized has reached ~4.2%, much higher than both ~1.58% of ZnO NW DSC and ~1.31% of ZnO NP DSC, prepared and tested under otherwise identical conditions. © *2010 American Institute of Physics*. [doi:10.1063/1.3327339]

Dye-sensitized solar cells (DSCs) have attracted a lot of attention as they are low-cost third generation solar cells, potentially for wide-spread commercialization.[1–3] The key element in DSC is the photoelectrode, which consists of highly porous wide band gap semiconductors, typically TiO_2 and ZnO network with dye molecules adsorbed onto the surface forming a monolayer. Dye molecules capture the incident photons and generate electron–hole pairs; electrons are readily injected into the conduction band of TiO_2 or ZnO and transported to charge collector. In order to achieve high power conversion efficiency (PCE), a large amount of dye molecules should be adsorbed, so a high specific surface area is desired. The charge transfer from dye molecules to charge collector should be efficient so as to minimize or eliminate possible loss of charges through surface recombination. Based on the TiO_2 nanoparticle (NP) network, the DSC has achieved AM 1.5 solar efficiencies more than 10%.[4,5] However, the further enhancement in PCE is difficult, partly due to charge recombination and reduced electron transport rate through the nanocrystalline photoanodes.[6] Efforts have been made to improve the charge transport in the photoelectrode, and the enhancement has been demonstrated by using one-dimensional nanostructure, including ZnO nanorod and nanowire (NW) and TiO_2 nanotube arrays.[6–9] However, the PCE of such DSC remained low, for example, ZnO NW DSC with the NW length as long as 33 μm was only 2.1% (Ref. 10) and a key point which limited the PCE of ZnO NW DSC should be an insufficient surface area for dye adsorption.[6]

The further improved the PCE of the DSC can be expected by making the photoanodes with exhibited both a high surface area and fast electron transport. Various ZnO structures have been employed to be used as photoanode of the DSC to improve the surface area and electron transport, including branch structure,[11] tetrapod,[12] nanoflower,[13] and composite NW/NP.[14–16] The overall PCE of these cells were largely increased, compared to pure ZnO NP DSC, which amounted to 1.51%, 3.27%, 1.9%, and 3.2% for branch structure, tetrapod, nanoflower, and composite ZnO NW/NP, respectively. The increase in the overall PCE is due to the enriched surface area for better dye loading and higher charge transport.[16,17] In this work, we report on the fabrication and investigation of DSC using ZnO NP and NW array photoanode (hybrid ZnO NW-NP DSC). The ZnO hybrid photoanode composed of ~11 μm length ZnO NW arrays to serve as a direct pathway for fast electron transport and crystallite ZnO NPs dispersed between ZnO NWs to offer a high surface area for dye adsorption.

Figure 1 is the scanning electron microscopy (SEM) images with Fig. 1(a) showing the top-view and Fig. 1(b) the cross-section of ZnO NW arrays. Details of a synthesis of

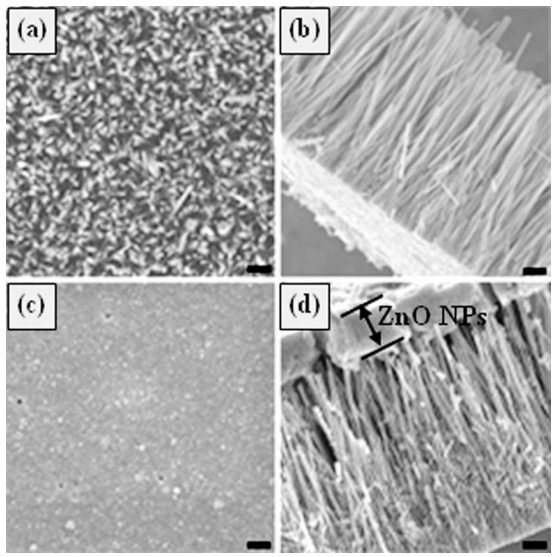

FIG. 1. SEM images of ZnO NW arrays and hybrid ZnO NW-NP, (a) the top-view of ZnO NW arrays, (b) cross-section of ZnO NW arrays, (c) top-view of hybrid ZnO NW-NP, and (d) cross-section of hybrid ZnO NW-NP. Scale bars in [(a)–(d)] are 1 μm.

a)Author to whom correspondence should be addressed. Electronic mail: gzcao@u.washington.edu.

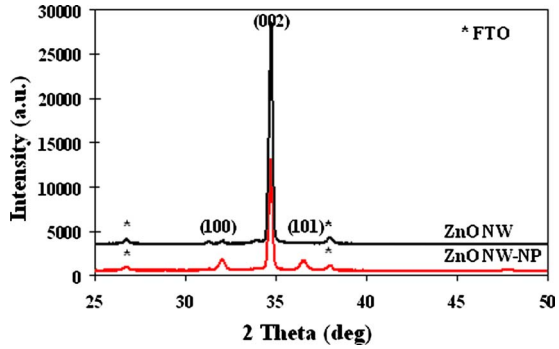

FIG. 2. (Color online) XRD patterns of ZnO NW and hybrid ZnO NW-NP.

ZnO NW arrays can be found elsewhere.[6,18,19] In brief, the ~100 nm thick seed layer was first prepared on the fluorine-doped tin oxide (FTO) glass substrates by spin-coat 0.60 mol l^{-1} of $Zn(CH_3COO)_2 \cdot 2H_2O$ in a 2-methoxyethanol/monoethanolamine. The seed substrates were annealed at 250 °C for 10 min, and subsequent soaking in an aqueous solution of 0.015 M $Zn(NO_3)_2$ and 0.015 M hexamethylenetetramine at 95 °C for 60 h with refreshing the growth solution every 12 h. The ZnO NWs with a diameter in the range of 40–500 nm (average ~116 nm) and a length of ~11 μm were well aligned perpendicularly to the FTO substrate. From SEM images, the density of ZnO NWs is estimated to be ~14 wires/μm^2. By spin-coating the colloidal dispersion of ZnO NPs (synthesized in diethylene glycol at 240 °C) on the top of ZnO NW arrays, the ZnO NPs with the average diameter of about 14 nm were partly penetrated and dispersed between of the ZnO NWs but with the large fraction remained and coated on the surface of NW arrays [shown in Figs. 1(c) and 1(d)].

Figure 2 shows and compares the XRD patterns of the ZnO NW film and hybrid ZnO NW-NP photoanode. ZnO NW-NP film exhibited a high crystallinity with very well defined (100), (002), and (101) diffraction peaks. The (002) diffraction peak is mainly attributed to the wurtzite structure of well aligned ZnO NWs which tend to occur along the c-axis.[20] The (100) and (101) diffraction peaks are resulted from the ZnO NPs.[21]

Figure 3 shows the photocurrent density (I)–voltage (V) characteristics for the DSC fabricated using N3-sensitized ZnO NPs, ZnO NWs, and hybrid ZnO NW-NP. The values of short-circuit current density (J_{sc}), open-circuit voltage (V_{oc}), fill factor (FF), and overall PCE (η), were summarized in Table I. The PCE of ZnO NW DSC with the length of ~1.7, 5.1, and 11 μm were 0.94%, 1.16%, and 1.58%, respectively. The increase in efficiency with the length of NW was the result of increase the surface area for dye absorption. However, there is no linear dependence between the PCE

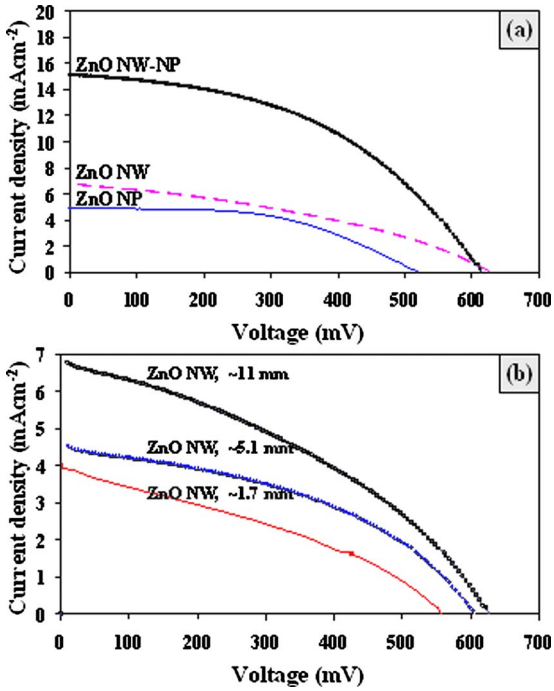

FIG. 3. (Color online) The photocurrent density-voltage curves of the N3-sensitized; (a) ZnO NP DSC, ZnO NW DSC, and hybrid ZnO NW-NP DSC and (b) ZnO NW DSC with the lengths of ~1.7, 5.1, and 11 μm.

and the length of ZnO NWs. Such a lack of direct relationship may be partly ascribed to the fact that the density of the NWs decreases with an increased length as a result of evolution selection growth. Reduced density of NWs would lead to a reduced surface area for dye adsorption. The obtained V_{oc} and FF of ZnO NW DSCs are comparable to Law *et al.*[6] and Xu *et al.*[10] The best overall PCE of DSC with the ZnO hybrid photoanode has reached 4.2% with V_{oc} of 613 mV, J_{sc} of 15.16 mA/cm^2, and a FF of 46%, far higher than both 1.58% of ZnO NW DSC, and 1.31% of ZnO NP DSC which prepared and tested under otherwise identical conditions.

The remarkable improved solar cell performance of ZnO NW-NP hybrid DSC was the results from the increase in J_{sc} and FF, which may be attributed to the following reasons. First, high-crystalline ZnO NPs (~14 mm) dispersed between long ZnO NW arrays (~11 μm) resulted in an increased surface area for more dye adsorption and, thus, an increased J_{sc}.[14,15,17] The amount of dye molecules adsorbed on ZnO NW and hybrid ZnO NW-NP photoelectrodes, by desorbing the dye molecules using a 0.1 M aqueous NaOH solution was found to be 6.39×10^{16} and 7.48×10^{16} molecule/cm^2, respectively. These results agree very well with the results reported by Rao and Dutta[22] and Seow *et al.*;[23] which showed the number of dye molecules ad-

TABLE I. The photovoltaic properties of ZnO DSCs.

Samples	The thickness of DSC (μm)	J_{sc} (mA/cm^2)	V_{oc} (mV)	FF (%)	η (%)
ZnO NW	~1.7 (NW)	4.09	553	41	0.94
ZnO NW	~5.1 (NW)	4.55	609	41	1.16
ZnO NW	~11 (NW)	6.79	629	37	1.58
ZnO NP	~10 (NP)	4.94	521	51	1.31
Hybrid ZnO NW-NP	~11+~2 (NW+NP)	15.16	613	46	4.24

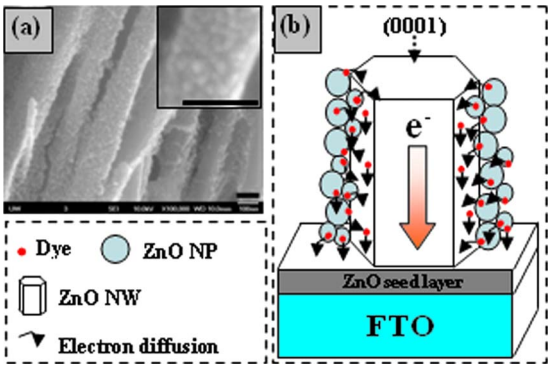

FIG. 4. (Color online) (a) The SEM image of ZnO NPs on the surface of ZnO NW in the hybrid ZnO NW-NP photoanode, scale bars 100 nm and (b) the schematic representation of the possible electron path way in the hybrid ZnO NW-NP photoanode.

sorbed on the ZnO NW surface is greater than that on the ZnO NP surface. Second, the single crystalline ZnO NWs in the hybrid ZnO NW-NP photoanode served as direct pathways for rapid charge transfer and consequently reduce the loss of charges as suggested in the open literature.[9,16] Schematic representation of the possible electron path way for the hybrid ZnO NW-NP DSC shows in Fig. 4(b). Finally, the increase in adsorbed-dyes on the ZnO NPs covered on the surface of ZnO NWs, as shown in Fig. 4(a), provides a sufficient electron which can compensate the sacrificing electron during the electron transport and, thus, improve the FF. It is also noted that although ZnO NWs in micrometer length may serve as light scatters as reported with large aggregates[24–26] or particles,[27] the significant enhancement of short circuit current density only in hybrid ZnO NW-NP photoanode DSC is unlikely due to the scattering effect. Further experiments are under way to improve the penetration of ZnO NPs between the ZnO NWs to further enhance the PCE.

In summary, the hybrid ZnO NW-NP photoanode for DSC has been fabricated and investigated to improve the PCE. The hybrid photoanode composed of ZnO NW arrays to serve as a direct pathway for fast electron transport and ZnO NPs dispersed and filled the gaps between ZnO NWs to offer a high surface area for sufficient dye adsorption. The overall PCE of DSC with the N3-sensitized ZnO hybrid photoanode has reached ~4.2%, with V_{oc} of ~613 mV, J_{sc} of ~15.2 mA/cm^2, and a FF of ~46%, far higher than ~1.58% of ZnO NW DSC, and ~1.31% of ZnO NP DSC, prepared and tested under otherwise identical conditions and all without chemical modification nor antireflection coating. The remarkably improved solar cell performance is attributed mainly to the improvement in J_{sc} which can be explained by the high surface area and fast electron transport of ZnO hybrid photoanodes.

This work has been supported by the Institute for the Promotion of Teaching Science and Technology (IPST), the Center of Excellence for Innovation in Chemistry (PERCH-CIC) (S.Y.), the U.S. Department of Energy, Office of Basic Energy Sciences, Division of Materials and Engineering under Award No. DE-FG02-07ER46467 (Q.F.Z.), the Air Force Office of Scientific Research (AFOSR-MURI, FA9550-06-1-0326) (K.S.P.), the University of Washington TGIF grant (X.Y.Z.), the Washington Research Foundation (C.S.D.), and the Intel Corporation.

[1]B. O'Regan and M. Grätzel, Nature (London) **353**, 737 (1991).
[2]M. K. Nazeeruddin, F. De Angelis, S. Fantacci, A. Selloni, G. Viscardi, P. Liska, S. Ito, B. Takeru, and M. Grätzel, J. Am. Chem. Soc. **127**, 16835 (2005).
[3]Q. F. Zhang, C. S. Dandeneau, X. Y. Zhou, and G. Z. Cao, Adv. Mater. (Weinheim, Ger.) **21**, 4087 (2009).
[4]M. Grätzel, Inorg. Chem. **44**, 6841 (2005).
[5]Q. Wang, S. Ito, M. Grätzel, F. Fabregat-Santiago, I. Mora-Sero, J. Bisquert, T. Bessho, and H. Imai, J. Phys. Chem. B **110**, 25210 (2006).
[6]M. Law, L. E. Greene, J. C. Johnson, R. Saykally, and P. Yang, Nature Mater. **4**, 455 (2005).
[7]E. Galoppini, J. Rochford, H. Chen, G. Saraf, Y. Lu, A. Hagfeldt, and G. Boschloo, J. Phys. Chem. B **110**, 16159 (2006).
[8]S. H. Kang, H. S. Kim, J. Y. Kim, and Y. E. Sung, Nanotechnology **20**, 355307 (2009).
[9]A. B. F. Martinson, M. S. Goes, F. Fabregat-Santiago, J. Bisquert, M. J. Pellin, and J. T. Hupp, J. Phys. Chem. A **113**, 4015 (2009).
[10]C. Xu, P. Shin, L. Cao, and D. Gao, J. Phys. Chem. C **114**, 125 (2010).
[11]H. M. Cheng, W. H. Chiu, C. H. Lee, S. Y. Tsai, and W. F. Hsieh, J. Phys. Chem. C **112**, 16359 (2008).
[12]W. Chen, H. Zhang, I. M. Hsing, and S. Yang, Electrochem. Commun. **11**, 1057 (2009).
[13]C. Y. Jiang, X. W. Sun, G. Q. Lo, D. L. Kwong, and J. X. Wang, Appl. Phys. Lett. **90**, 263501 (2007).
[14]J. B. Baxter and E. S. Aydil, Sol. Energy Mater. Sol. Cells **90**, 607 (2006).
[15]C. H. Ku and J. J. Wu, Nanotechnology **18**, 505706 (2007).
[16]C. H. Ku and J. J. Wu, Appl. Phys. Lett. **91**, 093117 (2007).
[17]Y. Wang, Y. Sun, and K. Li, Mater. Lett. **63**, 1102 (2009).
[18]J. Qiu, X. Li, W. He, S. J. Park, H. K. Kim, Y. H. Hwang, J. H. Lee, and Y. D. Kim, Nanotechnology **20**, 155603 (2009).
[19]L. E. Greene, B. D. Yuhas, M. Law, D. Zitoun, and P. Yang, Inorg. Chem. **45**, 7535 (2006).
[20]L. Vayssieres, Adv. Mater. **15**, 464 (2003).
[21]Y. Kim, H. Shang, and G. Cao, J. Sol-Gel Sci. Technol. **38**, 79 (2006).
[22]A. R. Rao and V. Dutta, Nanotechnology **19**, 445712 (2008).
[23]Z. L. S. Seow, A. S. W. Wong, V. Thavasi, R. Jose, S. Ramakrishna, and G. W. Ho, Nanotechnology **20**, 045604 (2009).
[24]Q. F. Zhang, T. P. Chou, B. Russo, S. A. Jenekhe, and G. Z. Cao, Angew. Chem. Int. Ed. **47**, 2402 (2008).
[25]Q. F. Zhang, T. P. Chou, B. Russo, S. A. Jenekhe, and G. Z. Cao, Adv. Funct. Mater. **18**, 1654 (2008).
[26]T. P. Chou, Q. F. Zhang, G. E. Fryxell, and G. Z. Cao, Adv. Mater. (Weinheim, Ger.) **19**, 2588 (2007).
[27]Z.-S. Wang, H. Kawauchi, T. Kashima, and H. Arakawa, Coord. Chem. Rev. **248**, 1381 (2004).